A Mouse Model of Diet-Induced Obesity Resembling Most Features of Human Metabolic Syndrome

Maria C. Della Vedova[1,2], Marcos D. Muñoz[1], Lucas D. Santillan[1–3], Maria G. Plateo-Pignatari[1], Maria J. Germanó[1], Martín E. Rinaldi Tosi[1], Silvina Garcia[1], Nidia N. Gomez[4], Miguel W. Fornes[5], Sandra E. Gomez Mejiba[2] and Dario C. Ramirez[1]

[1]Laboratory of Experimental and Translational Medicine, IMIBIO-SL, CONICET, National University of San Luis, San Luis, Argentina. [2]Laboratory of Experimental Therapeutics, IMIBIO-SL, CONICET, National University of San Luis, San Luis, Argentina. [3]Institute for Biochemical Research (INBIO), San Luis, Argentina. [4]Laboratory of Morphophysiology, IMIBIO-SL, CONICET, National University of San Luis, San Luis, Argentina. [5]LIAM, Andrology Research Laboratory from Mendoza, IHEM-CCT-Mendoza-National University of Cuyo, Mendoza, Argentina.

ABSTRACT: Increased chicken-derived fat and fructose consumption in the human diet is paralleled by an increasing prevalence of obesity and metabolic syndrome (MS). Herein, we aimed at developing and characterizing a mouse model of diet-induced obesity (DIO) resembling most of the key features of the human MS. To accomplish this, we fed male C57BL/6J mice for 4, 8, 12, and 16 weeks with either a low-fat diet (LFD) or a high-chicken-fat diet (HFD) and tap water with or without 10% fructose (F). This experimental design resulted in the following four experimental groups: LFD, LFD + F, HFD, and HFD + F. Over the feeding period, and on a weekly basis, the HFD + F group had more caloric intake and gained more weight than the other experimental groups. Compared to the other groups, and at the end of the feeding period, the HFD + F group had a higher adipogenic index, total cholesterol, low-density lipoprotein cholesterol, fasting basal glycemia, insulin resistance, hypertension, and atherogenic index and showed steatohepatitis and systemic oxidative stress/inflammation. A mouse model of DIO that will allow us to study the effect of MS in different organs and systems has been developed and characterized.

KEYWORDS: mouse model, diet-induced obesity, metabolic syndrome, adiposity, redox change, inflammation

CITATION: Della Vedova et al. A Mouse Model of Diet-Induced Obesity Resembling Most Features of Human Metabolic Syndrome. *Nutrition and Metabolic Insights* 2016:9 93–102 doi:10.4137/NMI.S32907.

TYPE: Original Research

RECEIVED: August 22, 2016. **RESUBMITTED:** October 31, 2016. **ACCEPTED FOR PUBLICATION:** November 2, 2016.

ACADEMIC EDITOR: Joseph Zhou, Editor in Chief

PEER REVIEW: Five peer reviewers contributed to the peer review report. Reviewers' reports totaled 1334 words, excluding any confidential comments to the academic editor.

FUNDING: This study was funded in part by fund from the Agencia Nacional para la Promoción de la Ciencia y la Tecnología-FONCyT (PICT-2014-3369), Universidad Nacional de San Luis (PROICO 2-3214 to DCR, PROICO 100414 to SEGM), and the Consejo Nacional de Investigaciones Científicas y Técnicas (PIP#2015-2017-112215-0100603CO to DCR and SEGM). The authors confirm that the funder had no influence over the study design, content of the article, or selection of this journal.

COMPETING INTERESTS: Authors disclose no potential conflicts of interest.

CORRESPONDENCE: ramirezlabimibiosl@ymail.com

Paper subject to independent expert single-blind peer review. All editorial decisions made by independent academic editor. Upon submission manuscript was subject to anti-plagiarism scanning. Prior to publication all authors have given signed confirmation of agreement to article publication and compliance with all applicable ethical and legal requirements, including the accuracy of author and contributor information, disclosure of competing interests and funding sources, compliance with ethical requirements relating to human and animal study participants, and compliance with any copyright requirements of third parties. This journal is a member of the Committee on Publication Ethics (COPE).

Provenance: the authors were invited to submit this paper.

Published by Libertas Academica. Learn more about this journal.

Introduction

Advances in technology have resulted in significant changes in the processing, availability, and composition of food.[1] Processed foods are enriched in saturated fat, *trans*-fatty acids, sucrose, fructose, and beef and soybean proteins, but they are poor in monounsaturated fatty acids (MUFAs), polyunsaturated fatty acids (PUFAs), plant-based proteins, and fiber.[1] According to the Food Agriculture Organization of the United Nations (FAO) and the Organization for Economic Co-operation and Development, the worldwide consumption of chicken has increased compared to the consumption of beef and pork. Compared to beef and pork, chicken meat has minor proportions of saturated fatty acids, but a high content of MUFAs and PUFAs.[2] In addition, currently, there is a tendency to consume drinks and food with a high energy value but poor in nutrients.[3] Fructose is commercially used as a sweetener (eg, corn syrup) and as a substitute for sucrose in the preparation of desserts, cakes, and carbonated drinks.[4]

The metabolic syndrome (MS) is one of the most serious consequences of overweight and obesity. This syndrome includes a number of metabolic obesity-associated abnormalities. MS is a constellation of clinical and biochemical key features that include central obesity, dyslipidemia, insulin resistance, hypertension, and nonalcoholic fatty liver (NAFL).[5,6] Patients with MS usually show a systemic pro-oxidant, pro-inflammatory, and pro-thrombotic profile linked to an increased risk of cardiovascular diseases, type 2 diabetes, NALF, osteoporosis, and premature death.[1,7–9] Recently, it has been suggested that the risk of MS is linked to hypercaloric diets with a high content of refined fats and carbohydrates.[10–15]

In order to understand the pathogenicity of obesity and obesity-associated metabolic complications, animal models are needed.[16] However, the major challenge is to find an animal model that develops more than two of the key features of human MS. Among the most used animal models of obesity are those with deficiency in the gene encoding leptin (*Ob/Ob* mice)[17] or leptin-receptor (*db/db* mice),[18] or other orexigenic genes. However, the fact that these gene deficiencies are rare human disorders raises concerns about the relevance of those models to human diseases. A number of diet-induced obesity

(DIO) models have been developed in rats and mice that have provided valuable information on the pathogenesis and therapeutics for obesity and obesity-associated metabolic complications.[16] DIO mouse models have been developed by feeding mice for 4–30 weeks with chow containing high fat and sugar, mostly sucrose, and in some cases fructose (F).[6,14,19–24] Models that utilize dietary extremes, such as 60% of calories from fat or 60% of calories from fructose, do not reflect commonly encountered dietary habits, and such dietary models typically focus on just one dietary component. A model resembling most of the key features of MS is needed in order to study the molecular mechanisms and therapeutics against this deadly syndrome associated with obesity and overweight.

Herein, we describe the experimental adjustment of a DIO model in male C57BL/6J mice based on feeding them food containing 22% (v/p) chicken-derived fat and 10% fructose in the drinking water. After 16 weeks of dieting, these mice developed dyslipidemia, insulin resistance, hypertension, NAFL-like histology, and systemic inflammation/oxidative stress. All these parameters resemble the human MS. Data gathered from this animal model can help us understand the pathogenesis and suggest therapeutics against MS.

Materials and Methods

Animal model. Six-week-old male C57BL/6J mice were used in this study. Mice were randomly divided into four groups and kept during the whole feeding period at a temperature of 23 ± 3°C with dark–light cycles of 12 hours. The four groups of six animals each were fed for 4, 8, 12, or 16 weeks as follows: LFD, mice were fed a low-fat diet and drank tap water; LFD + F, mice were fed an LFD and 10% fructose (*ENA Sport Nutrition*) (F) in tap water; HFD, mice were fed a high-fat diet and tap water; and HFD + F, mice were fed an HFD and 10% fructose in water. Food and drink were changed daily and provided ad libitum. Mouse chow was purchased from GEPSA S.A. and contained 6% chicken-derived fat, 40.7% carbohydrates, and 24% protein. The HFD was prepared in our laboratory by adding 22% chicken-derived fat (Granja Tres Arroyos). The final composition and caloric value of both diets, LFD and HFD, are shown in Table 1. All experiments were carried out according to a protocol approved by the Institutional Committee for Use of Animals in Research of the National University of San Luis (Protocol# B97/15) and followed the guidelines of the Guide for Care and Use of Laboratory Animals in Research (USNIH).

Table 1. Diet composition.*

	LFD	HFD
Moisture (%)	13.00	0.65
Ashes (%)	9.30	6.55
Fats (g%)	6.00	43.77
Crude fibers (g%)	7.00	6.52
Proteins (g%)	24.00	20.28
Carbohydrates (g%)	40.70	22.23
Energetic value (kcal%)	312.80	563.97

Note: *Fructose energy value: 3.9 kcal/mL.

Assessment of diet composition. To assess food moisture, 10 g of sample was weighed on a precision scale on a Petri dish and dried at 105 ± 1°C in a forced air oven until it attained a constant weight. Weight loss was considered to be the moisture content, and the dried residue was considered food-dry matter. The results were expressed as percentages.[25] For the determination of crude protein–nitrogen, the Kjeldahl procedure was followed.[26] The fat content in a food sample was measured using a Soxhlet extractor.[25] Ash content in the food was measured by a gravimetric method of previous calcination at 550 ± 25°C; the amount of residual inorganic matter was weighed, and results are shown as percentages.[25] The amount of crude fiber was determined following the Prosky method.[27] To assess the carbohydrate content in the food, FAO recommendations were followed. From the results of the determinations of fats (F), ashes (A), proteins (P), moisture (M), and dietary fibers (DF), the amount of carbohydrates was calculated as follows: carbohydrates (%) = 100 – (%F + %A + %P + %M + %DF).[25]

The energy value of the samples was obtained conveniently by adding the energy value from proteins, carbohydrates, and fats in each sample. To accomplish this, the following conversion factors were used according to Atwater numbers[28]: proteins = 4 kcal/g, carbohydrates = 4 kcal/g, and fats = 9 kcal/g.

Weight gain and calorie consumption. Food (g/day) and water (mL/day) consumption was measured every day for each 4 weeks of feeding. Total caloric intake (kcal/day) was calculated from the grams of food eaten and the milliliters of fluid drunk per day. Body weight gain (g) was recorded for each mouse from each group once a week during the entire feeding period (16 weeks).

Blood pressure measurements. Systolic blood pressure (SBP) and diastolic blood pressure (DBP) were measured every 4 weeks during the entire 16 weeks of feeding with a noninvasive tail-cuff system by using a CODA Surgical Monitor (Kent Scientific Co.). Measurements were performed and presented according to the manufacturer's instructions.

Glucose tolerance test. After 12 hours of fasting, mice were intraperitoneally injected with a 10% glucose solution at a dose of 2 g/kg. Blood glucose was measured using blood samples taken from a cut at the tail-tips at baseline (time = 0) and at 30, 60, and 120 minutes after the injection of glucose. Data are presented as glycemia curves.[29]

Euthanasia and tissue collection. At the end of the feeding period, animals were fastened for 12 hours and anesthetized with vapors of isofluorane. Blood was withdrawn following the submandibular vein (cheek-pouch) technique. After blood coagulation, the serum was collected for biochemical analysis. The epididymal fat depot was removed

following a surgical procedure and weighed. Adiposity index (AI%), a parameter of central obesity, was calculated using the following formula: [weight of epididymal fat pad(g)/body weight(g)] × 100.[19]

Adipokines, lipids, and markers of hepatic damage in serum. Serum leptin and adiponectin were measured using an enzyme-linked immunosorbent assay (ELISA) kit following the manufacturer's instructions (BioVision Inc.). Fasting serum triglyceride (TG), total cholesterol (TC), and high-density lipoprotein cholesterol (HDL-c) were measured using commercially available kits (Weiner Laboratories). Low-density lipoprotein cholesterol (LDL-c) was calculated as follows: LDL-c = [TC − TG/5] − HDL-c.[30] The atherogenic index (AI) was calculated using the following formula: TC (mg/dL)/HDL-c (mg/dL).[31] Glutamic oxaloacetic transaminase (GOT) and glutamic pyruvic transaminase (GPT), markers of hepatic function, were enzymatically measured by using a Wiener Autoanalyzer CM 250 and commercially available kits following the manufacturer's instructions (Wiener Laboratories). An internal quality control with levels 1 and 2 standards was performed.

Antioxidants in serum. Total antioxidant capacity (TAC) in serum was measured by an improved method that measures the quenching of the 2,2′-azino-bis-(3-ethylbenzothiazoline-6-sulfonic acid) radical cation ($ABTS^{\bullet+}$) by both lipophilic and hydrophilic antioxidants present in serum.[32] Reduced glutathione (GSH) concentration in serum was measured using a commercially available kit (Biovision Inc.). Oxidized glutathione (GSSG) was measured as GSH after treatment of the sample with GSH reductase following the manufacturer's instructions. Thiol status in serum is shown as the GSH/GSSG ratio.

Catalase (CAT)- and total glutathione peroxidase (GPx)-specific activities were measured as described using Aebi's[33] and Flohe and Gunzler's[34] methods, respectively. The results are expressed as international units per milligram of total proteins (IU/mg proteins).

Oxidative stress in serum. Lipid peroxidation was assessed spectrophotometrically by measuring thiobarbituric acid reactive substances (TBARS) at 535 nm.[35] The results are shown as µmol of malondialdehyde (MDA) per milligram of total proteins (µmol MDA/mg protein). Protein carbonyl content in serum proteins was measured using an ELISA as previously described.[36]

Nitrite assay. The concentration of nitrite in the serum was measured spectrophotometrically by using Griess reagents as previously described.[37] The results were expressed as nmol of nitrite per milligram of protein (nmol NO_2^-/mg protein).

Interluekin-6. Interluekin-6 (IL-6), a marker of inflammation, was measured in serum using a quantitative murine-IL-6 sandwich ELISA following the manufacturer's instructions (Cat# 900-k50, Peptrotech).

Histology. Paraffin liver sections of 5–6 µm thickness were cut and stained with hematoxylin–eosin (H&E). Histological observations were made on at least four sections of the different regions. Microphotographs were taken using an Olympus BX50 microscope connected to a digital camera and a PC-based image analysis system (Image J).[38]

Statistics. All data are shown as mean values ± standard error of the mean, with six mice from each group and from three independent experiments. All statistical comparisons were performed using the Student's *t*-test for independent groups and one-way analysis of variance for comparison of means of parameters within the same group at different times. *P*-values <0.05 were considered statistically significant.

Results

Diet composition. Table 1 shows the percentage composition of each diet used to feed animals. Fat content was seven times higher in HFD than LFD, whereas carbohydrate content was almost twice as much in LFD than in HFD, but all other components were only slightly modified. Most likely because of the high-fat content, the moisture of HFD was only 0.65%, whereas LFD had 13%. The energetic values of LFD and HFD diets were 312.8 and 536.97 kcal per 100 g of food, respectively. Fructose contributes 3.9 kcal per ml of a 10% fructose solution in tap water (Table 1).

HFD + F group consumes more calories. Table 2 shows food and drink consumption, as well as caloric intake, for each experimental group at 4, 8, 12, and 16 weeks of feeding. Food intake was not different among the four groups. Starting from the 4th week of feeding, fluid intake was higher in animals from the LFD + F, HFD, and HFD + F groups than the LFD group. Caloric intake per mouse was also assessed each 4 weeks of dieting and on a daily basis by measuring food and drink consumption. Compared to the LFD, animals from the other groups had a higher caloric intake starting from week 4 of dieting. During the 16th week of feeding, total caloric intake (kcal/day) was as follows: HFD + F (46.15 + 0.90) > LFD + F (37.27 + 0.88) > HFD (14.28 + 0.20) > LFD (9.21 + 0.22). These results show that at week 16, HFD + F animals consumed more fructose solution and ate an amount of food equal to the other experimental groups but consumed almost five times more kcal/day than the LFD group and approximately three times more than the HFD group.

HFD + F group gains more weight and adiposity. All mice started the experiment with similar body weight. The higher total caloric intake in the HFD + F group led to higher body weight gain (g) as compared with other experimental groups over a feeding period of 16 weeks (HFD + F, 36.55 ± 0.69; HFD, 31.55 ± 0.44; LFD + F, 28.31 ± 0.26; LFD, 27.36 ± 0.19, $P < 0.001$) (Fig. 1A). Interestingly, after 2 weeks of feeding, HFD + F animals gained more weight than any other animals ($P < 0.05$). Afterward, HFD + F gained more weight than any other group ($P < 0.01$). The greater differences started to be more notable after 6–7 weeks of feeding, when HFD + F and HFD animals started to gain more weight than the other

Table 2. Food, drink, and caloric intake.

	LFD	LFD + F	HFD	HFD + F
Week 4				
Food (g/day)	2.92 ± 0.24*	2.51 ± 0.06	2.95 ± 0.15	2.04 ± 0.23
Drink (mL/day)	4.56 ± 0.41	6.16 ± 1.91[a]	6.34 ± 3.57[a]	7.38 ± 2.04[a–c]
Caloric intake (kcal/day)	9.11 ± 0.20	31.8 ± 0.90[a]	16.60 ± 1.86[a,b]	40.26 ± 1.13[a–c]
Week 8				
Food (g/day)	2.87 ± 0.35	2.60 ± 0.20	2.60 ± 0.11	2.08 ± 0.05
Drink (mL/day)	3.69 ± 1.05	8.34 ± 1.41[a]	2.13 ± 0.42[a,b]	9.5 ± 1.82[a,c]
Caloric intake (kcal/day)	8.90 ± 0.71	40.63 ± 0.80[a]	14.63 ± 0.26[a,b]	48.76 ± 0.93[a–c]
Week 12				
Food (g/day)	2.57 ± 0.44	1.87 ± 0.22[a]	2.46 ± 0.26[b]	1.46 ± 0.21[a,c]
Drink (mL/day)	5.04 ± 1.19	7.09 ± 1.25[a]	6.31 ± 1.92[a]	7.18 ± 2.16[a,c]
Caloric intake (kcal/day)	8.01 ± 0.81	33.48 ± 0.73[a]	13.84 ± 1.09[a,b]	36.22 ± 1.18[a–c]
Week 16				
Food (g/day)	2.95 ± 0.07	2.35 ± 0.06	2.55 ± 0.03	2.16 ± 0.05
Drink (mL/day)	4.52 ± 0.26	7.65 ± 0.47[a]	4.95 ± 0.56[b]	8.71 ± 0.46[a,c]
Caloric intake (kcal/day)	9.21 ± 0.22	37.27 ± 0.88[a]	14.28 ± 0.20[a,b]	46.15 ± 0.90[a–c]

Notes: *Values are presented as mean values ± standard error of the mean. Statistical symbols ([a]LFD, [b]LFD + F, [c]HFD) show differences at $P < 0.05$, n = 6.
Abbreviations: LFD, low-fat diet; LFD + F, low-fat diet with fructose in drinking water; HFD, high-fat diet; HFD + F, high-fat diet with fructose in drinking water.

animals. The images in Figure 1A (insert) show a distinctive epididymal adipose depot in a representative animal from each experimental group. The weight of the epididymal fat depot (g) was higher in the HFD + F group as compared to the other three groups (HFD + F, 1.36 ± 0.10; HFD, 0.91 ± 0.07; LFD + F, 0.54 ± 0.04; LFD, 0.36 ± 0.02) (Fig. 1B). The adiposity index (AI%), a marker of central adiposity, was higher in the HFD + F group than any of the other groups (HFD + F, 3.89 ± 0.24; HFD, 2.89 ± 0.20; LFD + F, 1.88 ± 0.13; LFD, 1.32 ± 0.10) (Fig. 1C).

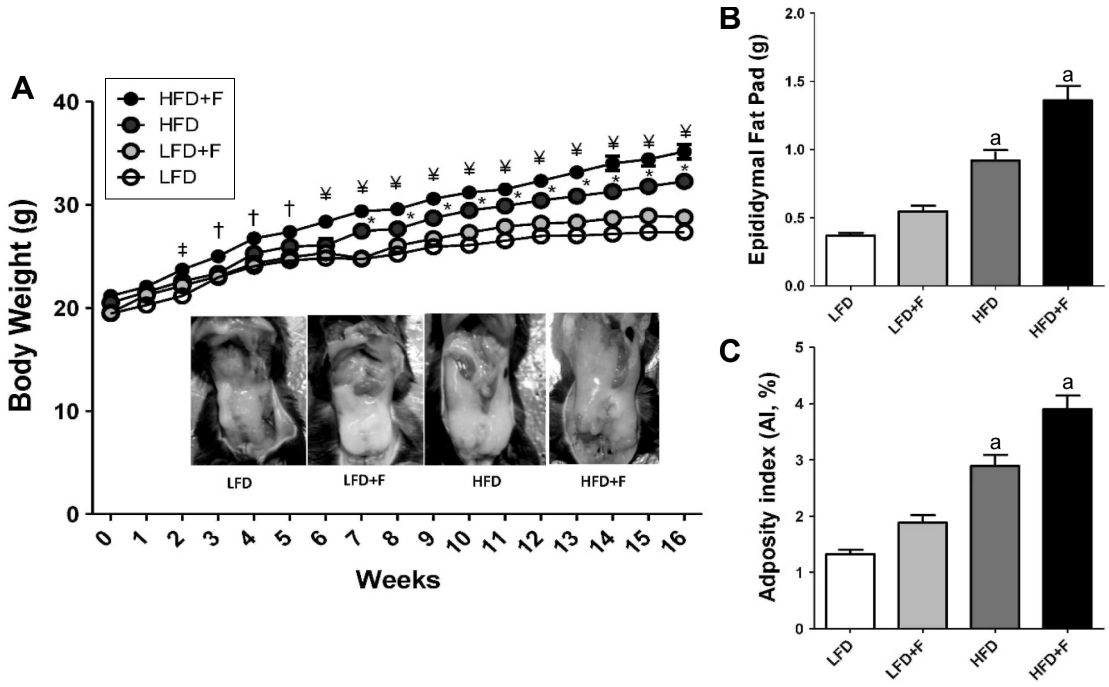

Figure 1. HFD + F diet induces central adiposity in mice. (**A**) Body weight gain curve in C57BL/6J mice fed for 4, 8, 12, and 16 weeks an LFD and HFD with (LFD + F and HFD + F) or without fructose in the drinking water. $^{‡}P < 0.05$, $^{¥}P < 0.01$, and $^{†}P < 0.001$ compared HFD + F with LFD. *Indicates differences ($P < 0.05$) between HFD and LFD. Insert, epididymal fat depot in a representative mouse from each group after 16 weeks of dieting. (**B**) Weight of epididymal fat depot after 16 weeks of feeding. (**C**) Adiposity index (AI%): [(epididymal fat/body weight) × 100]. Results are shown as representative images or mean values ± standard error of the mean (n = 6). $^{a}P < 0.05$ compared to LFD.

HFD + F group develops more hypertension. To assess hypertension, we measured changes in SBP and DBP in each experimental group after 4, 8, 12, and 16 weeks of dieting (Fig. 2). No changes in blood pressure were observed before 12 weeks of feeding (Fig. 2A and B). However, starting from the 12th week of feeding and as compared to animals fed either an LFD, LFD + F, or HFD, animals fed an HFD + F had higher DBP and SBP (Fig. 2C). Figure 2D shows that the HFD + F group had a higher SBP and DBP than the other experimental groups (HFD + F, 203.0 ± 4.5/167.4 ± 3.0; HFD, 162.3 ± 2.9/127.6 ± 3.6; LFD + F, 157.4 ± 2.4/131.8 ± 1.9; LFD, 142.6 ± 2.5/115.8 ± 3.8). After 16 weeks of feeding, animals from the LFD + F and HFD groups had higher SBP than the LFD group. Although SBP and DBP were not significantly different between the HFD and LFD + F groups, the animals who consumed the most calories had the highest DBP and SBP after a feeding period of 16 weeks.

HFD + F group develops insulin resistance. To assess insulin sensitivity, we measured fasting blood glucose and performed a glucose tolerance test (GTT) in animals from each group at 4, 8, 12, and 16 weeks of feeding. Fasting blood glucose (mg/dL) was higher in the HFD + F group than in the other experimental groups (HFD + F, 181.8 ± 24.0; HFD, 144.2 ± 15.7; LFD + F, 113.5 ± 15.2; LFD, 110.5 ± 6.8) (Fig. 3A). Starting from the 8th week of feeding, animals fed with an HFD had higher blood fasting glycemia than animals fed an LFD. Moreover, the GTT shows that HFD + F mice had impairment in glucose disposal after an intraperitoneal injection (Fig. 3B). Although all groups reached a glycemic peak at 30 minutes postglucose challenge (HFD + F, 396.3 ± 26.9; HFD, 372.7 ± 23.3; LFD + F, 328.5 ± 30.8; LFD, 308.0 ± 5.7), the glucose concentration (mg/dL) at 60–120 minutes postglucose injection was higher in the HFD + F group as compared to other experimental groups (60/120 minutes: HFD + F, 308.3 ± 19.6/197.7 ± 22.8; HFD, 245.0 ± 22.0/172.2 ± 20.7; LFD + F, 229.7 ± 36.0/160.0 ± 19.9; LFD, 191.2 ± 5.6/123.3 ± 16.2).

Systemic oxidative stress in the HFD + F group. Table 3 shows the assessment of systemic redox status in animals fed for 16 weeks with the four experimental diets. Serum TAC was measured as a parameter of antioxidant content that may change by depletion of antioxidants due to increased detoxification of pro-oxidants and inflammation.[39] Serum from HFD + F animals had a reduced TAC as compared to the

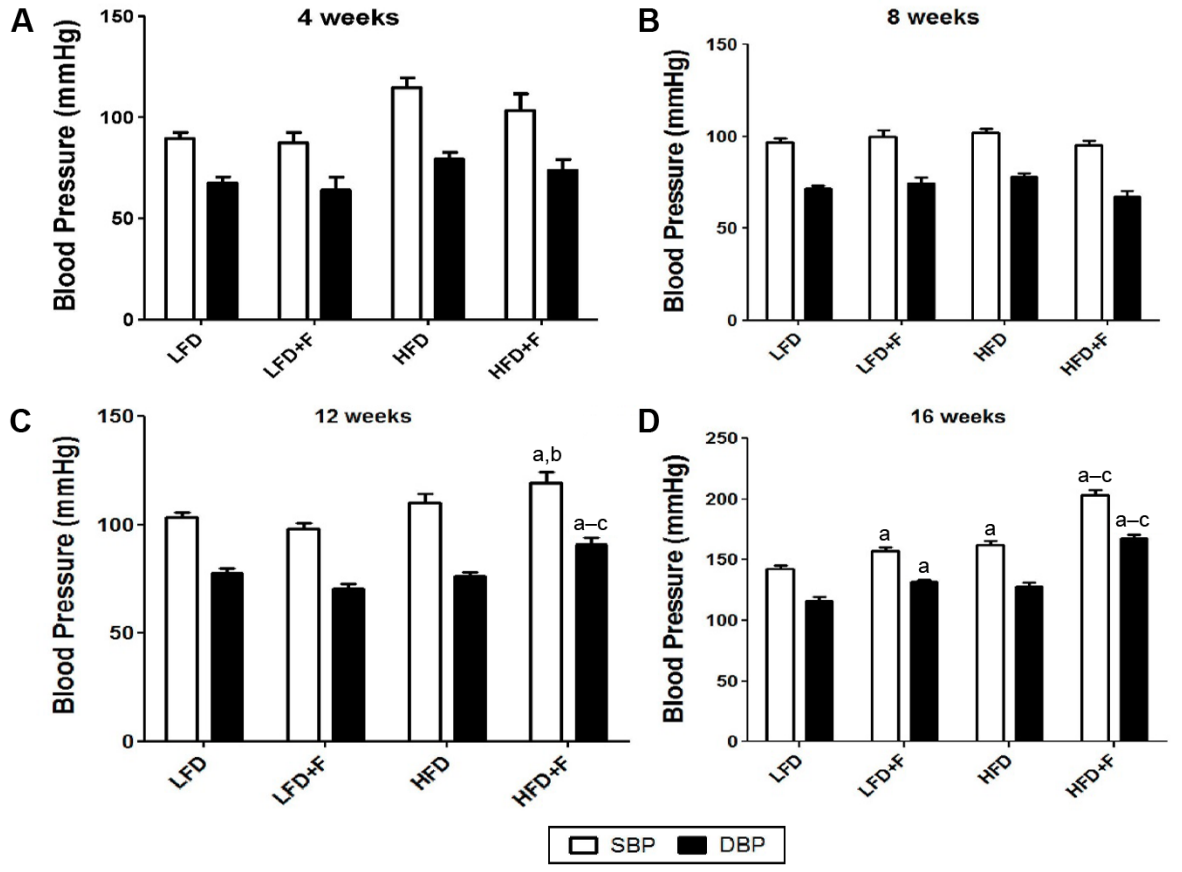

Figure 2. HFD + F diet feeding elevates SBP in C57BL/6J mice. Mice were fed LFD—low-fat diet; LFD + F—low-fat diet with fructose in drinking water; HFD—high-fat diet; HFD + F—high-fat diet with fructose in drinking water for 4 (**A**), 8 (**B**), 12 (**C**), and 16 (**D**) weeks. At the end of the feeding period, SBP and DBP were measured as indicated in the "Materials and methods" section. The values are reported as mean ± standard error of the mean (n = 6). $^{a–c}P < 0.05$ compared to LFD, LFD + F, and HFD + F, respectively.

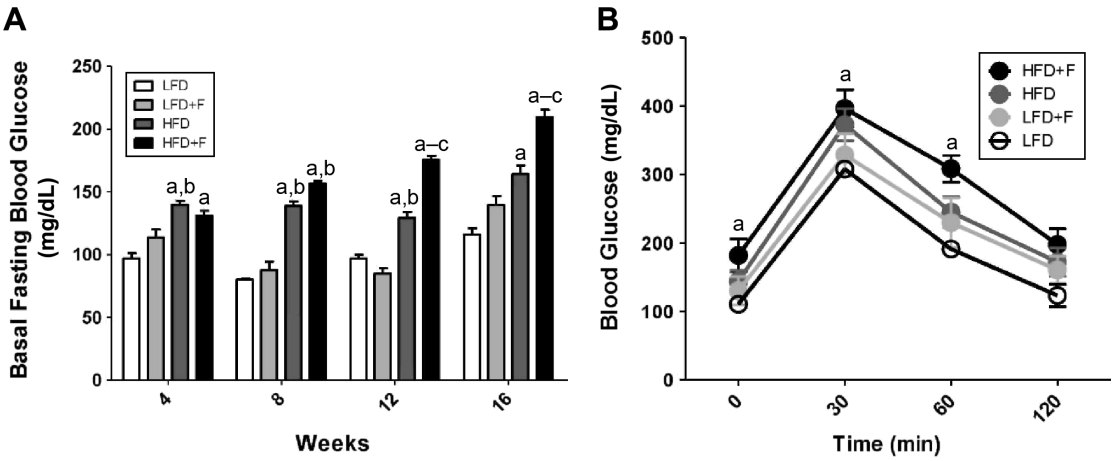

Figure 3. HFD + F induces insulin resistance in mice. (**A**) The basal fasting glycemia was determined after 4, 8, 12, and 16 weeks of feeding. [a–c]$P < 0.05$ compared to LFD, LFD + F, and HFD + F, respectively. (**B**) GTT was performed at 16 weeks of feeding for each experimental group of animals. [a]Indicates differences ($P < 0.05$) compared with the LFD group. The values are shown as mean ± standard error of the mean, n = 6.

LFD + F and LFD groups. HFD animals showed reduced TAC as compared to LFD and LFD + F animals. Animals from the HFD + F group had less TAC than HFD animals. To assess systemic nonenzymatic antioxidant defenses, the GSH/GSSG ratio was measured in serum. The GSH/GSSG ratio was diminished in the serum of HFD + F mice as compared to all other experimental mice ($P < 0.001$). To assess enzymatic antioxidants in serum, we measured the specific activity of CAT and GPx. Serum CAT and GPx activity was higher in the HFD + F group than in the other three experimental groups ($P < 0.001$).

Lipid peroxidation, a marker of lipid oxidation, was measured as TBARS (Table 3). Serum TBARS were increased in the serum of animals from the HFD + F group as compared to any of the other experimental groups ($P < 0.001$). HFD caused increased TBARS in serum when compared to LFD. There was no change in serum TBARS when LFD and LFD + F were compared. Serum carbonyls, markers of protein oxidation, were higher in HFD + F mice than in the other three experimental groups. Compared to LFD, all the other experimental groups showed at least twice the protein carbonyl concentration in serum.

Systemic inflammation is affected by the diet. Serum nitrites and IL-6 were measured in the serum as markers of systemic inflammation. Figure 4A shows that, compared to other groups, nitrite concentration (nmol/mg protein) was higher in mice fed an HFD + F (HFD + F: 16.9 ± 2.6; HFD: 10.1 ± 1.4; LFD + F: 8.1 ± 1.1; LFD: 4.6 ± 0.9). The concentration of IL-6 in serum (pg/mL) was more than twice as high in HFD + F than in any other experimental group (HFD + F) (Fig. 4B). No differences in serum IL-6 were observed between the LFD, LFD + F, and HFD experimental groups.

Dyslipidemia is only observed in the HFD + F group. To assess systemic biochemical status, we measured the changes in the concentration of adipokines, lipid profiles, and markers of liver status in the serum of mice fed with different diets. As shown in Table 4, HFD and HFD + F caused increased leptin but reduced adiponectin concentrations

Table 3. Systemic redox status.

	LFD	LFD + F	HFD	HFD + F
Antioxidants				
TAC (μM ascorbic acid)	2,478.00 ± 103.80*	2,419.00 ± 107.60	2,115.00 ± 54.7[a]	1,799.00 ± 37.10[a,b]
GSH/GSSG ratio	128.70 ± 0.70	97.77 ± 1.50[a]	50.63 ± 2.70[a,b]	28.54 ± 5.10[a–c]
CAT (IU/mg protein)	17.43 ± 1.50	29.33 ± 0.60[a]	30.89 ± 0.70[a]	42.13 ± 2.60[a–c]
GPx (IU/mg protein)	0.12 ± 0.01	0.26 ± 0.08[a]	0.29 ± 0.05[a]	0.36 ± 0.09[a–c]
Markers of oxidative stress				
TBARS (μmol/mg protein)	0.16 ± 0.01	0.21 ± 0.06	0.25 ± 0.08[a]	0.3 ± 0.03[a–c]
Carbonyls (nmol/mg protein)	0.75 ± 0.20	1.40 ± 0.03[a]	1.4 ± 0.10[a]	2.03 ± 0.09[a–c]

Notes: *Values are presented as mean ± standard error of the mean. Statistical symbols ([a]LFD, [b]LFD + F, [c]HFD) show differences, $P < 0.05$. n = 6.
Abbreviations: LFD, low-fat diet; LFD + F, low-fat diet with fructose in drinking water; HFD, high-fat diet; HFD + F, high-fat diet with fructose in drinking water; TAC, total antioxidant capacity; GSH, reduced glutathione; GSSG, oxidized glutathione; CAT, catalase; GPx, glutathione peroxidase; TBARS, thiobarbituric acid reactive substances.

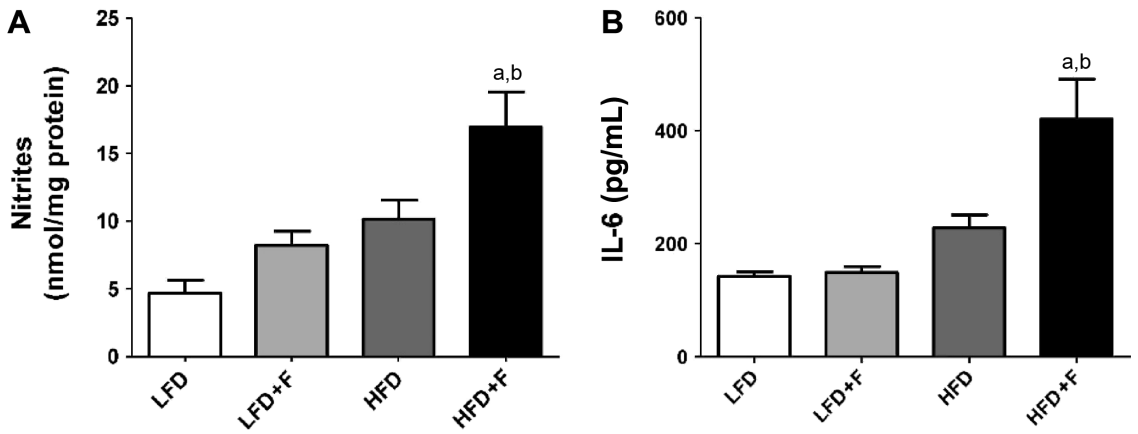

Figure 4. Markers of systemic inflammation in serum. (**A**) Serum nitrites are shown as nmol/mg proteins. (**B**) Serum IL-6 was determined by a quantitative ELISA as indicated in the "Materials and methods" section. Results are shown as mean values ± standard error of the mean. $^{a,b}P < 0.05$ compared to LFD and LFD + F, respectively. Repeated measures analysis of variance followed by the Bonferroni test was used.

in serum. Comparing all groups, the highest and lowest concentrations of leptin and adiponectin, respectively, were found in the serum of the HFD + F mice. Along with serum nitrites and IL-6, this profile of adipokines indicates systemic inflammation and an insulin-desensitizing status. Compared to the LFD group, TC only increased in the serum of the HFD + F group. Interestingly, and compared to the LFD group, serum concentration of TG increased in the HFD and HFD + F groups. HDL-c diminished and LDL-c increased only in the HFD + F group when compared with the other three groups. These data suggest a marked dyslipidemia—a feature of MS herein only observed in the HFD + F group. This lipid profile is compatible with a higher atherogenic index (AI)—a parameter of visceral adiposity. Indeed, AI was higher in the HFD + F group than any other experimental groups.

To assess liver status, we measured the serum concentration of GOT and GPT (Table 4). Animals from the HFD + F group showed the highest concentration of GPT, but interestingly, this group showed a reduced concentration of GOT.

HFD + F group develops steatohepatitis. To relate biochemical data to liver status, liver histopathology was performed in each experimental group (Fig. 5). H&E-stained cuts were analyzed at low (10×) and then at higher (600×) magnification for evidence of injury and steatosis. Liver histology of LFD (Fig. 5A) shows normal architecture. There were no appreciable differences between LFD and LFD + F liver histology (Fig. 5B). The light micrographs in LFD + F showed the most hepatocytes having a light eosinophilic cytoplasm. Significant morphological changes in hepatic parenchyma were observed in mice fed with HFD and HFD + F for

Table 4. Biochemical parameters in serum.

	LFD	LFD + F	HFD	HFD + F
Adipokines				
Leptin (pg/mL)	244.0 ± 44.7*	284.0 ± 68.7	424.0 ± 64.2	577.0 ± 92.1[a,b]
Adiponectin (pg/mL)	565.5 ± 91.7	418.7 ± 87.7	345.3 ± 68.1	265.5 ± 61.2[a]
Serum lipids				
Total cholesterol (mg/dL)	153.0 ± 2.6	161.0 ± 3.4	175.0 ± 8.0	192.0 ± 2.0[a]
Triglycerides (mg/dL)	129.7 ± 4.3	131.0 ± 4.8	167.3 ± 4.0	210.3 ± 6.3[a]
HDL-c (mg/dL)	46.2 ± 3.4	34.0 ± 2.7	46.0 ± 2.1	34.2 ± 0.8[a]
LDL-c (mg/dL)	39.2 ± 1.6	52.3 ± 5.5	54.2 ± 10.1	63.9 ± 5.7[a]
Atherogenic index	3.4 ± 0.3	4.6 ± 0.4	3.8 ± 0.1	5.6 ± 0.1[a]
Liver status				
GOT (IU/L)	119.3 ± 14.0	87.6 ± 1.4	84.6 ± 10.0	66.0 ± 14.5[a]
GPT (IU/L)	36.0 ± 3.2	48.0 ± 6.3	54.0 ± 4.0	64.0 ± 7.8[a]

Notes: *Values are shown as mean values ± standard error of the mean. Statistical symbols ([a]LFD, [b]LFD + F, [c]HFD) show differences, $P < 0.05$, n = 6.
Abbreviations: LFD, low-fat diet; LFD + F, low-fat diet with fructose in drinking water; HFD, high-fat diet; HFD + F, high-fat diet with fructose in drinking water; HDL-c, high-density lipoprotein cholesterol; LDL-c, low-density lipoprotein cholesterol; atherogenic index = (total cholesterol/HDLc); GOT, glutamic oxaloacetic transaminase; GTP, glutamic–pyruvic transaminase.

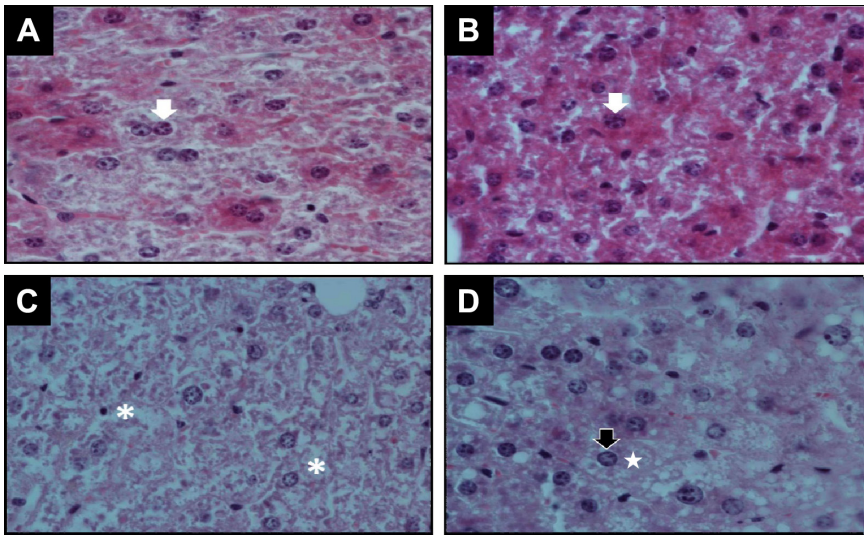

Figure 5. Histopathological changes in the liver. Representative photograph of H&E staining (600×) of liver sections from each group of animals: (**A**) LFD, (**B**) LFD + F, (**C**) HFD, and (**D**) HFD + F after 16 weeks of feeding. Normal bi- or monogranulated nucleus (white arrows) inside an eosinophilic cytoplasm of hepatocytes was observed in LFD (**A**) and LFD + F (**B**). Instead, loosened (white asterisk in **C**, HFD) or vacuolated cytoplasm (white stars in **D**, HFD + F) associated with a nuclear displacement (black arrow) is observed in the liver of animals fed with HFD + F.

16 weeks (Fig. 5C and D). The hepatic cells from HFD + F-fed mice showed degenerative changes in shape and low affinity for stains, which is compatible with increased lipid content that is lost during the processing of the sample (Fig. 5D).

HFD + F liver shows ballooned hypochromic hepatocytes with cytosolic membrane-delimited droplets indicating hypertrophy of the smooth endoplasmic reticulum due to TG accumulation (steatosis) with marginalization of the nucleus. Moreover, diffuse acidophilic bodies in cytoplasm are present in this group (H&E staining, 600×). However, livers of HFD mice showed less vacuolated cytoplasm (steatosis) than the HFD + F group (compare Fig. 5C and D).

Discussion

Herein, an animal model resembling some of the key features of the human MS has been developed. B6 male mice were fed either an LFD or an HFD for 16 weeks and tap water with or without 10% fructose. The uniqueness of this model is the addition of chicken-derived fat instead of either bovine- or porcine-derived fat. Mice fed with an HFD + F for 16 weeks developed most of the key features of the human MS including central obesity, dyslipidemia, hypertension, insulin resistance, systemic oxidative stress/inflammation, and steatohepatitis. Male mice were chosen for this model because of their higher susceptibility than female mice to adipose tissue oxidative stress and inflammation[40]—key processes connecting the many features of human MS. Moreover, male mice do not have hormonal changes related to estrous stages, which may affect biochemical parameters.

There are several animal models used to study obesity and obesity-associated metabolic abnormalities. However, the most appropriate is the use of inbred strains of mice that gain weight by manipulation of the environment instead of genetics.[16] The standard Western diet has a high content of fat and sugar, which makes it energy rich. This combination is considered to be the main cause of DIO, obesity-associated comorbidities, and MS.[1,14,22] The C57BL/6J mouse-strain is one of the most appropriate mouse strains because it shows, from the first week of the diet, a higher weight gain when fed an HFD.[23,24] In this study, we show that mice fed a combination of chicken fat in the diet and fructose in the drinking water, as observed in the American diet, develop most of the key features of MS.

Patients with MS have been shown to consume around 10–15% of fructose in their diets, and thus, our model may be nonrelevant; however, this may provide critical information to analyze organ-specific effects of MS and will help find novel targets for intervention.[14,23] The uniqueness of our HFD + F model of MS is the combination of chicken-derived fat in the food and fructose in the drinking water. Interestingly, fructose in drinking water reduced food consumption; however, total caloric intake in animals fed an HFD + F was higher than in the HFD group. Our study agreed with a number of previous studies showing that animals fed a diet rich in either fat or fructose gain more weight than control animals.[9,14,24,41–43] To assess the contribution of chicken-derived fat in the food to MS, we measured the key features of MS in animals fed four different diets. Comparing weight gain and adiposity between the HFD and LFD + F groups, we found that HFD mice are heavier than LFD + F mice; however, the latter had a higher energy uptake than the first. This may reflect the fact that fructose did not induce insulin release from pancreatic β-cells. β-Cells have a low expression of the fructose transporter, glucose transporter-5 (GLUT-5), which limits their ability to

sense fructose concentration.[1,4] Moreover, chronic HFD consumption alters insulin signaling, which results in adiposity by inducing expression of critical lipogenic enzymes.[4]

The visceral adipose tissue depot, which can be effectively assessed by the adiposity index (AI%), is the central feature of MS and relates to systemic inflammation.[44] In mice, the epididymal adipose depot is one of the major visceral depots that makes up total adiposity, adipose tissue inflammation, and systemic inflammation. Hypertrophic and hyperplastic adipose tissues become inflamed by recruitment and differentiation of monocytes to macrophages.[45] At the inflammation, site macrophages acquire an inflammatory M1-phenotype causing adipose tissue inflammation.[45] Adipose tissue inflammation is one of the major sources of low-grade chronic systemic oxidative stress and inflammation.[46] Our study shows that a combination of chicken-derived fat and fructose in the diet causes loss or reduction of insulin sensitivity in the HFD + F group as compared to the other experimental groups. It has been reported that hypercaloric diets reduce insulin sensitivity, but the mechanism has not been elucidated.[22,24,47–49]

Increased secretion of pro-oxidative, pro-inflammatory, and insulin-desensitizing adipokines by inflamed adipose tissue has been suggested as the central mechanism of hypertension in obesity and MS.[14,50–52] Indeed, our data show that HFD + F and HFD groups have hyperleptinemia and hypoadiponectinemia, which is in agreement with previous reports.[22,53] Because of the hyperleptinemia observed in these groups, we rationalized that these animals have a state of brain leptin resistance,[54] and thus, further leptin response experiments would not provide any valuable additional information. It is also known that dietary fructose induces leptin expression, whereas it reduces adiponectin expression.[23–51] This effect of fructose may be amplified by the consumption of chicken-derived fat in the food.

Although many organs are targets of systemic oxidative stress and inflammation, NAFL is one of the better studied features of MS in humans. Our data showed that after 16 weeks of feeding an HFD with or without fructose in the water caused a marked hypochromic pattern in the H&E stain, suggesting that stain is removed during sample preparation due to the high content of TG. The pattern of lipid accumulation inside hepatocytes in the HFD + F is in droplets surrounded by a membrane, resembling a hyperplasic endoplasmic reticulum due to TG accumulation. Caloric excess and further metabolic inflammation, oxidative stress, and insulin resistance are the central mechanisms of NAFL in MS.[55–57] Our data showed systemic oxidative stress and inflammation and a marked dyslipidemia in the HFD + F and HFD groups.

The serum of mice fed with HFD + F showed a reduced TAC. This finding suggests that feeding animals with fructose and chicken-derived fat causes a reduction in antioxidants, for example, GSH, free thiol groups in proteins, uric acid, and L-ascorbate. Indeed, increased reactive species production is thought to be produced by activated inflammatory cells at the hypertrophied and inflamed adipose tissue.[44] Oxidative stress is the damage to macromolecules resulting from an imbalance between pro-oxidants and antioxidants, in favor of the former. To assess systemic oxidative stress and inflammation, we measured protein carbonyls—a marker of protein oxidation—and TBARS—a marker of lipid peroxidation. Protein carbonyls and TBARS were increased in the serum of HFD + F > HFD, whereas there was no difference between the HFD versus LFD + F, suggesting that neither fructose nor chicken-derived fat alone is enough to cause systemic oxidative stress. Besides adipokine imbalance toward pro-inflammation, nitrite and IL-6 in serum—two markers of systemic inflammation—increased in HFD + F when compared with the other experimental groups.

Concluding Remarks

Herein, we developed and characterized a mouse model that exhibits most of the feature of the human MS. C57BL/6J mice fed with food enriched in chicken-derived fat and drinking water with fructose shows central adiposity, insulin resistance, hypertension, and liver steatosis resembling some key features of human MS. This animal model will help to dissect the pathogenesis of MS in different tissues as well as providing a useful tool to study novel therapeutics.

Acknowledgments

Authors are deeply grateful to the members of the Laboratory of Food Sciences, School of Engineering and Agrarian Sciences, led by Teresa Malka for determination of the composition of the diet.

Author Contributions

Conceived and designed the experiments: MCDV, MDM, MJG, LDS, MGPP, MERT, SG, SEGM and DCR. Analyzed the data: MCDV, NNG, SEGM and DCR. Wrote the first draft of the manuscript: MCDV, SEGM, NNG and DCR. Contributed to the writing of the manuscript: MCDV, MWF, NNG, SEGM and DCR. Agree with manuscript results and conclusions: MCDV, NNG, SEGM and DCR. Jointly developed the structure and arguments for the paper: MCDV, NNG, MWF, SEGM and DCR. Made critical revisions and approved final version: MCDV, NNG, SEGM and DCR. All authors reviewed and approved of the final manuscript.

REFERENCES

1. Odermatt A. The Western-style diet: a major risk factor for impaired kidney function and chronic kidney disease. *Am J Physiol Renal Physiol*. 2011;301(5):F919–F931.
2. Hernandez Rodriguez M, Gallego Sastre A. *Tratado de Nutrición*. Madrid, Spain. Ediciones Diaz de Santos, S.A. 1999;1(Chapter 1):3–39.
3. Ludwig DS. Dietary glycemic index and obesity. *J Nutr*. 2000;130(2S suppl):280S–283S.
4. Elliott SS, Keim NL, Stern JS, Teff K, Havel PJ. Fructose, weight gain, and the insulin resistance syndrome. *Am J Clin Nutr*. 2002;76(5):911–922.
5. Tran LT, Yuen VG, McNeill JH. The fructose-fed rat: a review on the mechanisms of fructose-induced insulin resistance and hypertension. *Mol Cell Biochem*. 2009;332(1–2):145–159.

6. Mamikutty N, Thent ZC, Sapri SR, Sahruddin NN, Mohd Yusof MR, et al. The establishment of metabolic syndrome model by induction of fructose drinking water in male Wistar rats. *Biomed Res Int*. 2014;2014263897.
7. Kalupahana NS, Claycombe KJ, Moustaid-Moussa N. (n-3) Fatty acids alleviate adipose tissue inflammation and insulin resistance: mechanistic insights. *Adv Nutr*. 2011;2(4):304–316.
8. Brown CM, Dulloo AG, Montani JP. Sugary drinks in the pathogenesis of obesity and cardiovascular diseases. *Int J Obes (Lond)*. 2008;32(suppl 6):S28–S34.
9. Kulkarni NM, Jaji MS, Shetty P, Kurhe YV, Chaudhary S, et al. A novel animal model of metabolic syndrome with non-alcoholic fatty liver disease and skin inflammation. *Pharm Biol*. 2015;53(8):1110–1117.
10. Welsh JA, Sharma A, Abramson JL, Vaccarino V, Gillespie C, et al. Caloric sweetener consumption and dyslipidemia among US adults. *JAMA*. 2010;303(15):1490–1497.
11. Ruxton CH, Gardner EJ, McNulty HM. Is sugar consumption detrimental to health? A review of the evidence 1995–2006. *Crit Rev Food Sci Nutr*. 2010;50(1):1–19.
12. Dekker MJ, Su Q, Baker C, Rutledge AC, Adeli K. Fructose: a highly lipogenic nutrient implicated in insulin resistance, hepatic steatosis, and the metabolic syndrome. *Am J Physiol Endocrinol Metab*. 2010;299(5):E685–E694.
13. Vasdev S, Longerich L, Gill V. Prevention of fructose-induced hypertension by dietary vitamins. *Clin Biochem*. 2004;37(1):1–9.
14. Lozano I, Van der Werf R, Bietiger W, Seyfritz E, Peronet C, et al. High-fructose and high-fat diet-induced disorders in rats: impact on diabetes risk, hepatic and vascular complications. *Nutr Metab (Lond)*. 2016;13:15.
15. Nakagawa T, Tuttle KR, Short RA, Johnson RJ. Hypothesis: fructose-induced hyperuricemia as a causal mechanism for the epidemic of the metabolic syndrome. *Nat Clin Pract Nephrol*. 2005;1(2):80–86.
16. Tschop M, Heiman ML. Rodent obesity models: an overview. *Exp Clin Endocrinol Diabetes*. 2001;109(6):307–319.
17. Friedman JM, Halaas JL. Leptin and the regulation of body weight in mammals. *Nature*. 1998;395(6704):763–770.
18. Coleman DL. Obese and diabetes: two mutant genes causing diabetes-obesity syndromes in mice. *Diabetologia*. 1978;14(3):141–148.
19. Nascimento TB, Baptista Rde F, Pereira PC, Campos DH, Leopoldo AS, et al. Vascular alterations in high-fat diet-obese rats: role of endothelial L-arginine/NO pathway. *Arq Bras Cardiol*. 2011;97(1):40–45.
20. Yang ZH, Miyahara H, Takeo J, Katayama M. Diet high in fat and sucrose induces rapid onset of obesity-related metabolic syndrome partly through rapid response of genes involved in lipogenesis, insulin signalling and inflammation in mice. *Diabetol Metab Syndr*. 2012;4(1):32.
21. Martins MA, Catta-Preta M, Mandarim-de-Lacerda CA, Aguila MB, Brunini TC, et al. High fat diets modulate nitric oxide biosynthesis and antioxidant defence in red blood cells from C57BL/6 mice. *Arch Biochem Biophys*. 2010;499(1–2):56–61.
22. Lee JS, Jun DW, Kim EK, Jeon HJ, Nam HH, et al. Histologic and Metabolic Derangement in High-Fat, High-Fructose, and Combination Diet Animal Models. *Scientific World Journal*. 2015;2015306326.
23. Aydin S, Aksoy A, Kalayci M, Yilmaz M, Kuloglu T, et al. Today's and yesterday's of pathophysiology: biochemistry of metabolic syndrome and animal models. *Nutrition*. 2014;30(1):1–9.
24. Zhuhua Z, Zhiquan W, Zhen Y, Yixin N, Weiwei Z, et al. A novel mice model of metabolic syndrome: the high-fat-high-fructose diet-fed ICR mice. *Exp Anim*. 2015;64(4):435–442.
25. Association of Official Analytical Chemists International. *Animal fed*. In: Official Methods of Analysis of OAOC International. 15th ed. Rockville, MD, USA: AOAC INTERNATIONAL. 1990;1(Chapter 4):1–77.
26. Ma TZ, Micro-Kjeldahl G. Determination of Nitrogen. A New Indicator and An Improved Rapid Method. *Ind Eng Chem Anal*. 1942;14(3):280–282.
27. Prosky L, Asp NG, Furda I, DeVries JW, Schweizer TF, et al. Determination of total dietary fiber in foods and food products: collaborative study. *J Assoc Off Anal Chem*. 1985;68(4):677–679.
28. FAO United Nations. *Calculation of the energy content of foods-energy conversion factors*. In: FAO Food and Nutrition Paper 77. Rome: Agriculture and Consumer Protection. 2002;Chapter 4:18–58.
29. Andrikopoulos S, Blair AR, Deluca N, Fam BC, Proietto J. Evaluating the glucose tolerance test in mice. *Am J Physiol Endocrinol Metab*. 2008;295(6):E1323–E1332.
30. Marvin Querales MID, Susan Rojas. Estimación del colesterol LDL a través de la ecuación brasilera: comparación con otras metodologías. *Rev Latinoam Patol Clin Med Lab*. 2015;62(2):91–96.
31. Nwagha UI, Ikekpeazu EJ, Ejezie FE, Neboh EE, Maduka IC. Atherogenic index of plasma as useful predictor of cardiovascular risk among postmenopausal women in Enugu, Nigeria. *Afr Health Sci*. 2010;10(3):248–252.
32. Re R, Pellegrini N, Proteggente A, Pannala A, Yang M, et al. Antioxidant activity applying an improved ABTS radical cation decolorization assay. *Free Radic Biol Med*. 1999;26(9–10):1231–1237.
33. Aebi H. Catalase in vitro. *Methods Enzymol*. 1984;105:121–126.
34. Flohe L, Gunzler WA. Assays of glutathione peroxidase. *Methods Enzymol*. 1984;105:114–121.
35. Draper HH, Hadley M. Malondialdehyde determination as index of lipid peroxidation. *Methods Enzymol*. 1990;186:421–431.
36. Winterbourn CC, Buss IH. Protein carbonyl measurement by enzyme-linked immunosorbent assay. *Methods Enzymol*. 1999;300:106–111.
37. Moshage H, Kok B, Huizenga JR, Jansen PL. Nitrite and nitrate determinations in plasma: a critical evaluation. *Clin Chem*. 1995;41(6 Pt 1):892–896.
38. Abramoff MD MP, Ram SJ. Image Processing with Image J. *Biophotonics International*. 2004;11(7):36–42.
39. Halliwell B. Establishing the significance and optimal intake of dietary antioxidants: the biomarker concept. *Nutr Rev*. 1999;57(4):104–113.
40. Nickelson KJ, Stromsdorfer KL, Pickering RT, Liu TW, Ortinau LC, et al. A comparison of inflammatory and oxidative stress markers in adipose tissue from weight-matched obese male and female mice. *Exp Diabetes Res*. 2012;2012859395.
41. Coate KC, Kraft G, Lautz M, Smith M, Neal DW, et al. A high-fat, high-fructose diet accelerates nutrient absorption and impairs net hepatic glucose uptake in response to a mixed meal in partially pancreatectomized dogs. *J Nutr*. 2011;141(9):1643–1651.
42. Panchal SK, Brown L. Rodent models for metabolic syndrome research. *J Biomed Biotechnol*. 2011;2011351982.
43. Wada T, Kenmochi H, Miyashita Y, Sasaki M, Ojima M, et al. Spironolactone improves glucose and lipid metabolism by ameliorating hepatic steatosis and inflammation and suppressing enhanced gluconeogenesis induced by high-fat and high-fructose diet. *Endocrinology*. 2010;151(5):2040–2049.
44. Hotamisligil GS, Shargill NS, Spiegelman BM. Adipose expression of tumor necrosis factor-alpha: direct role in obesity-linked insulin resistance. *Science*. 1993;259(5091):87–91.
45. Lee J. Adipose tissue macrophages in the development of obesity-induced inflammation, insulin resistance and type 2 diabetes. *Arch Pharm Res*. 2013;36(2):208–222.
46. Shapiro H, Lutaty A, Ariel A. Macrophages, meta-inflammation, and immunometabolism. *Scientific World Journal*. 2011;11:2509–2529.
47. Coate KC, Scott M, Farmer B, Moore MC, Smith M, et al. Chronic consumption of a high-fat/high-fructose diet renders the liver incapable of net hepatic glucose uptake. *Am J Physiol Endocrinol Metab*. 2010;299(6):E887–E898.
48. Kershaw EE, Flier JS. Adipose tissue as an endocrine organ. *J Clin Endocrinol Metab*. 2004;89(6):2548–2556.
49. Havel PJ. Dietary fructose: implications for dysregulation of energy homeostasis and lipid/carbohydrate metabolism. *Nutr Rev*. 2005;63(5):133–157.
50. Bjorntorp P. Adipose tissue distribution and function. *Int J Obes*. 1991;15(suppl 2):67–81.
51. Cao H. Adipocytokines in obesity and metabolic disease. *J Endocrinol*. 2014;220(2):T47–T59.
52. Lumeng CN, Bodzin JL, Saltiel AR. Obesity induces a phenotypic switch in adipose tissue macrophage polarization. *J Clin Invest*. 2007;117(1):175–184.
53. Benetti E, Mastrocola R, Rogazzo M, Chiazza F, Aragno M, et al. High sugar intake and development of skeletal muscle insulin resistance and inflammation in mice: a protective role for PPAR-delta agonism. *Mediators Inflamm*. 2013;2013509502.
54. Lin S, Thomas TC, Storlien LH, Huang XF. Development of high fat diet-induced obesity and leptin resistance in C57Bl/6J mice. *Int J Obes Relat Metab Disord*. 2000;24(5):639–646.
55. Coate KC, Huggins KW. Consumption of a high glycemic index diet increases abdominal adiposity but does not influence adipose tissue pro-oxidant and antioxidant gene expression in C57BL/6 mice. *Nutr Res*. 2010;30(2):141–150.
56. Shoelson SE, Herrero L, Naaz A. Obesity, inflammation, and insulin resistance. *Gastroenterology*. 2007;132(6):2169–2180.
57. Stanhope KL, Havel PJ. Endocrine and metabolic effects of consuming beverages sweetened with fructose, glucose, sucrose, or high-fructose corn syrup. *Am J Clin Nutr*. 2008;88(6):1733S–1737S.